ICAS 2016
30th Congress of the International Council of the Aeronautical Sciences
DCC, Daejeon, Korea ; September 25-30, 2016

ON APPLYING PISTON THEORY IN INTERFERENCE FLOWS

Marius-Corne Meijer* , **Laurent Dala*,**** , **Peter G. Karkle*****
***University of Pretoria,** ****Council for Scientific and Industrial Research,** *****Central Aerohydrodynamic Institute**

Keywords: *wing-body interference, piston theory, approximate modelling, slender body*

Abstract

The theoretical basis for applying piston theory to a slender wing-body combination is considered and a numerical example is given with comparison to experimental data and other prediction methods.

1 Introduction

Piston theory [1] has long been used to predict surface pressures on wings and on panels in supersonic flows. Classical piston theory (CPT) is defined by modelling perturbations relative to the freestream flow. It has been extended to account for upstream influence in the case of airfoils and flat panels [2], and to account for curvature in the case of shells with no crossflow [3]. CPT has also been used to add nonlinear thickness effects to otherwise linear panel methods [4] and to estimate the effective airfoil shape in hypersonic flows due to the boundary layer displacement thickness [5]. Local piston theory [6] (LPT) is defined by modelling perturbations relative to an existing mean steady-state solution. LPT applied relative to Euler solutions has seen increased use due to its associated reduction of computational cost relative to full unsteady Euler solution, and has recently seen increased application to vehicles [7] rather than to isolated surfaces. The accuracy of the Euler-based LPT results has seen to be lower [7] when applied to vehicles with aerodynamically interfering components than when applied to isolated surfaces. This, along with the recent application of LPT relative to Navier-Stokes solutions [8], has motivated the present investigation into the basis for the application of piston theory to interference flows.

2 Theoretical basis

Piston theory is a special case of the unsteady analogy, which relates the steady (or unsteady) flow in N dimensions to the unsteady flow in $N-1$ dimensions – in particular, at hypersonic speeds, this is known as the hypersonic equivalence principle. Various milestones in the reduction of the order of the equations for slender bodies have been achieved, with notable contributions due to Ilyushin [9] at low incidences and due to Sychev [10] at high incidences. A summary of the various similitudes and their relation to each other is given in [11]. It has been found [12] that in certain cases, the similitudes (such as Sychev's [10]) correlate well with experimental data well outside of the limiting assumptions imposed in their theoretical derivation.

Piston theory may be derived from the Euler equations when the ratios of certain lengths or gradients and velocities in the flow become small parameters and the associated terms are discarded. In particular, piston theory requires that gradients in two orthogonal directions be neglected, as illustrated in Fig. 1, where as the unsteady analogy and other related methods typically only require gradients along the body axis to be neglected. A mathematical treatment of these considerations and the conditions under which they break down is given in [13]; here, the ideas will be illustrated by considering only one component of the momentum equation and considering typical crossflow-plane flowfields.

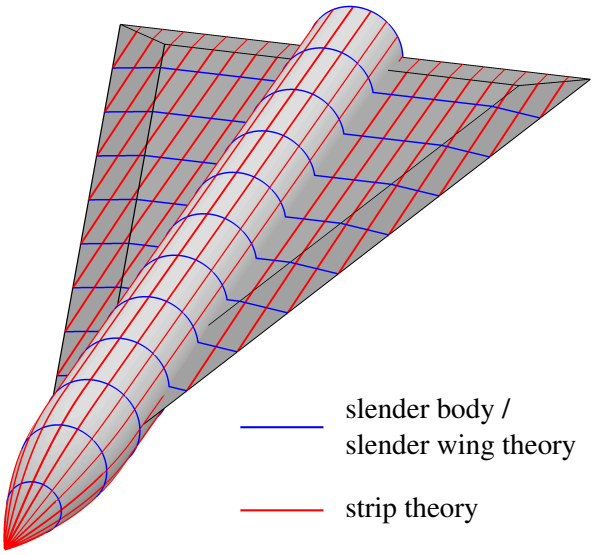

Fig. 1 : Planes normal to which gradients are neglected in piston theory.

Consider the third component of the momentum equation, with terms nondimensionalized with respect to reference values such that the terms and their derivatives are $O(1)$. The velocities u_i are referenced to values U_i, coordinates ξ_i are nondimensionalized with respect to lengths L_i, and the dimensionless pressure p and density ρ have reference values p_R and ρ_R respectively:

$$\left(\frac{L_3U_1}{L_1U_3}\right)u_1\frac{\partial u_3}{\partial\xi_1}+\left(\frac{L_3U_2}{L_2U_3}\right)u_2\frac{\partial u_3}{\partial\xi_2}+ +u_3\frac{\partial u_3}{\partial\xi_3}=-\left(\frac{U_1^2}{U_3^2}\frac{p_R}{\rho_RU_1^2}\right)\frac{1}{\rho}\frac{\partial p}{\partial\xi_3} \quad (1)$$

The bracketed terms are dimensionless parameters of the local flow problem; for given magnitudes of these parameters, the order of magnitude of perturbations to u_i may be considered and a truncation up to a certain order of smallness may be made, potentially removing a variable u_i from the equation. The various methods that result from the unsteady analogy differ in the particulars of the order of the various dimensionless parameters and the order of the perturbations. Piston theory, as a point-function relation between pressure and velocity, requires the gradients in the ξ_1 and ξ_2-directions to be neglected. This effectively precludes its application in regions where the crossflow velocity or acceleration tangential to the surface is of the order of the piston velocity – this may occur in various regions in the flowfield as illustrated in Fig. 2, typically where significant surface curvature exists: the wing-body junction, the wing-tips, and potentially on the body surface in crossflow.

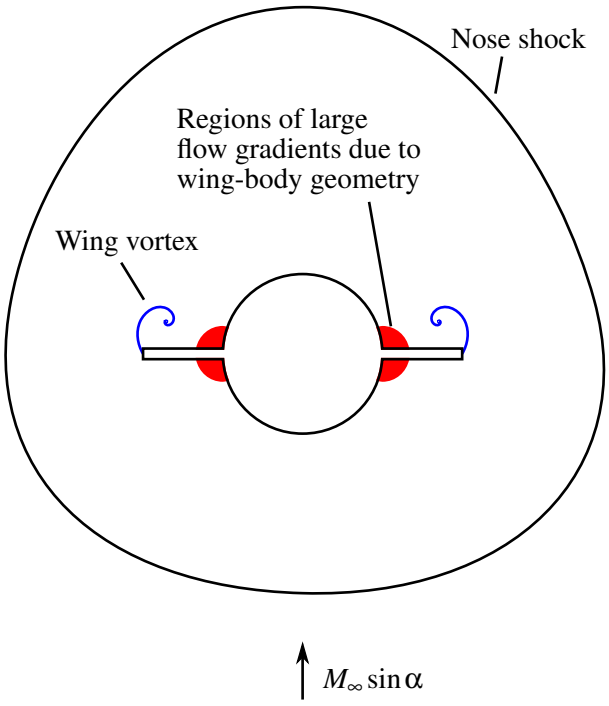

Fig. 2 : Typical flow in the crossflow plane at small incidence.

3 Application

The application of classical piston theory to a body with a monoplane wing is illustrated in this section. The geometry considered is described in Fig. 3, corresponding to the model geometry of a series of experimental work by Fellows & Carter [14]. The results presented in [14] are limited to the normal-force coefficient for the various model components across the spectrum of angle-of-attack (α) and freestream Mach number (M_∞); the pressure distribution at a given combination of M_∞ and α for all the components was not given. A systematic comparison to experiment of the pressure distribution predicted by piston theory was thus not possible. However, for the portion of the wing-body combination aft

of the wing root, a comparison of the normal-coefficients could be made for the combination (C_N), the interference of the wing on the body ($C_{N_{B(W)}}$), and for the wing including the interference from the body ($C_{N_{B(W)}}$). The values are related by:

$$C_N = C_{N_B} + C_{N_{B(W)}} + C_{N_{W(B)}} \qquad (2)$$

where C_{N_B} is the normal-force coefficient of the isolated body. The additional terms are related to the normal-force coefficient of the isolated wing (C_{N_W}) through carry-over factors $K_{B(W)}$ and $K_{W(B)}$:

$$C_{N_{B(W)}} = K_{B(W)} C_{N_W}, \quad C_{N_{W(B)}} = K_{W(B)} C_{N_W} \qquad (3)$$

It is important to note that in the following sections, C_N and $C_{N_{B(W)}}$ refer to the portion of the body aft of the root of the wing, and not to the entire body. The results from applying classical piston theory to the geometry are compared to those obtained from a public-domain version of the NASA-AMES WingBody panel code, as well as to experiment and approximate methods to model interference.

$(\frac{R}{D}) = 0.30984(\frac{x}{D}) - 0.03989(\frac{R}{D})^2 - 0.00261(\frac{R}{D})^3$

$L = 19.5$”, $D = 1.5$”, $L_N = 3D$

Common: $L_W = 14.384$”, $L_c = 0.75$”, $t = 0.202$”

Wing 1: $\Lambda_{LE} = 78.2°$, $s_W = 3$”

Wing 8: $\Lambda_{LE} = 85.5°$, $s_W = 1.125$”

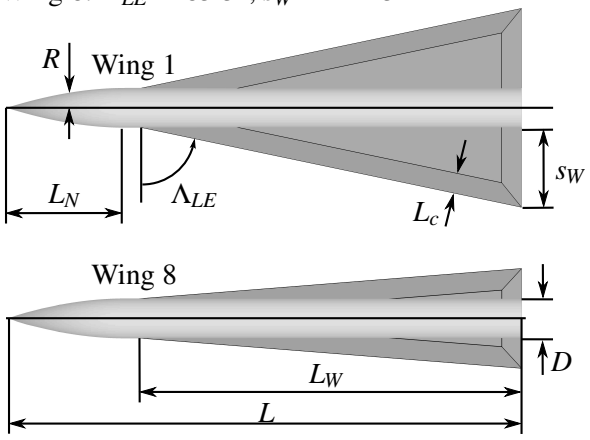

Fig. 3 : Geometry definition.

3.1 Reference Data and Methods

The experimental values of the normal-force coefficient were obtained in [14] by integration of the pressure distribution over the surfaces of the various model components – this allowed for the experimental $C_{N_{W(B)}}$ to be obtained directly; the value of $C_{N_{B(W)}}$ was deduced from the measured value of $C_{N_B} + C_{N_{B(W)}}$ and from tests of the isolated body (C_{N_B}). These results, along with values from various prediction methods, are shown in Figs. 5–10. The normal-force coefficient of the isolated wing (C_{N_W}) was also determined by experiment.

Fellows & Carter [14] applied the carry-over factors $K_{B(W)}$ and $K_{W(B)}$ to the experimentally-measured C_{N_W} to obtain predictions for the normal-force coefficient of the portion of the wing-body combination subject to interference. The values used for the carry-over factors were taken from slender body theory [15] (SBT), upwash theory [15] (UT), and the P-N-K method [15] (PNK), and are summarized in Table 1 and Table 2.

Table 1: Wing-on-body carry-over factor, $K_{B(W)}$

	Method	$M_\infty = 2.0$	$M_\infty = 2.8$
Wing 1	SBT	0.278	0.278
	PNK	0.246	0.232
Wing 8	SBT	0.611	0.611
	PNK	0.581	0.565

Table 2: Body-on-wing carry-over factor, $K_{W(B)}$

Method	Wing 1	Wing 8
SBT	1.162	1.349
UT	1.300	1.522

3.2 Piston Theory

Classical piston theory was used to obtain predictions for the isolated body (C_{N_B}) and the isolated wing (C_{N_W}); no attempt was made to model the interference, i.e., $C_{N_{B(W)}} = 0$ and $C_{N_{W(B)}} = C_{N_W}$. For reference, the normal-force coefficient of the nose alone was also computed for comparison to experiment; the results are

shown in Fig. 5 and Fig. 6. The coordinate system used in defining the downwash equations is shown in Fig. 4. The pressure coefficient as

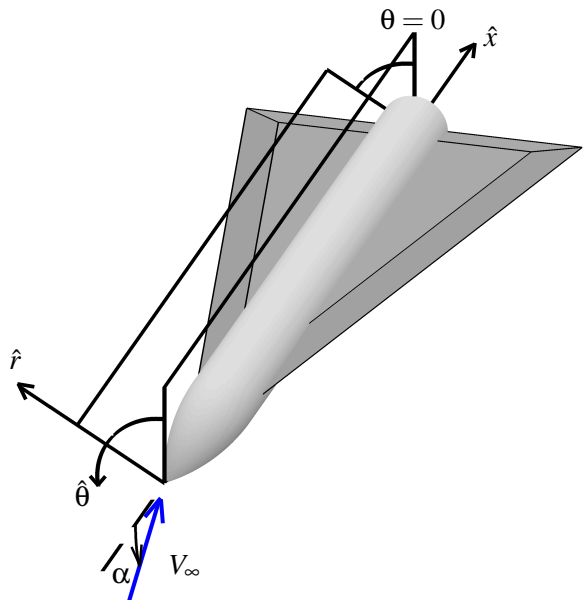

Fig. 4 : Coordinate system.

modelled by classical piston theory is given by:

$$C_P = \frac{2}{M_\infty}\left(c_1\hat{w} + c_2 M_\infty \hat{w}^2 + c_3 M_\infty^2 \hat{w}^3\right) \qquad (4)$$

in which $\hat{w}$ is the downwash nondimensionalized with respect to the freestream velocity, and for which the coefficients c_1, c_2, and c_3 are dependent on the pressure equation used. In the case of expansion, the limiting value of C_P corresponds to that at vacuum. The general expressions for the coefficients are given in [16]; for the present case the coefficients are listed in Table 3, and are seen to be close to those due to Lighthill [17].

Table 3: Piston theory pressure coefficients

	$M_\infty = 2.0$	$M_\infty = 2.8$
c_1	1.155	1.071
c_2	0.733	0.642
c_3, $\hat{w} > 0$	0.254	0.181
c_3, $\hat{w} \le 0$	0.234	0.185

The dimensionless downwash $\hat{w}$ is defined as:

$$\hat{w} \equiv -\hat{\mathbf{V}}_\infty \cdot \hat{\mathbf{n}} \qquad (5)$$

where $\hat{\mathbf{V}}_\infty$ is the unit vector of the freestream velocity and $\hat{\mathbf{n}}$ is the unit normal vector of the body or wing surface. The dimensionless downwash may be split into a component ($\hat{w}_a$) associated with surface gradients relative to the component of V_∞ directed along the axis of the body ($\hat{x}$-direction) and into a component ($\hat{w}_c$) associated with surface gradients relative to the component of V_∞ lying in the crossflow plane:

$$\hat{w} = \hat{w}_a + \hat{w}_c \qquad (6)$$

The unit normal vector of the surface for the body is given as:

$$\hat{\mathbf{n}} = -\sin\phi\,\hat{\mathbf{x}} + \cos\phi\sin\phi\,\hat{\mathbf{r}} + \cos\phi\cos\theta\,\hat{\boldsymbol{\theta}} \qquad (7)$$

In this formulation, the following relations hold:

$$\text{Body:} \quad \hat{w}_a = \cos\alpha\sin\phi \qquad (8)$$

$$\hat{w}_c = -\sin\alpha\cos\phi\cos\theta \qquad (9)$$

$$\text{Wing:} \quad \hat{w}_a \approx 0 \qquad (10)$$

$$\hat{w}_c \approx \begin{cases} -\sin\alpha, & \text{upper} \\ +\sin\alpha, & \text{lower} \end{cases} \qquad (11)$$

The normal-force coefficient is then obtained by integrating the pressure over the surface:

$$C_{N_B} = -\frac{1}{S_W}\int_0^{2\pi}\int_{L-L_W}^{L} C_P R\cos\phi\cos\theta\, d\theta\, dx \qquad (12)$$

$$C_{N_W} = -\frac{1}{S_W}\iint_{\text{wing}} C_P R\, dS \qquad (13)$$

In each case, the normal-force coefficient is referenced to the wing area (S_W) of the wing considered. The results obtained using 1st-order and 3rd-order piston theory with no interference modelling are shown in Figs. 5–10. It is noted that classical piston theory with the downwash equation as defined here produces a lifting pressure-distribution around the cylindrical portion of the body for all $\alpha \neq 0$.

4 Discussion

For a discussion on the results of slender body theory (SBT), the P-N-K method (PNK), and of

upwash theory (UT) and their correlation to the experimental results, the reader is referred to the report of Fellows & Carter [14]; here, it is only remarked that the departure of these results from the experimental data highlights the fact that the interference is not linear with α. The correlation of the WingBody panel code and of piston theory to the experimental results is discussed here, with reference to Figs. 5–10.

4.1 WingBody Code

Firstly, it is noted that all the results from the WingBody code are linear with α, as is expected for the linearized potential flow code. Fairly good correlation with experiment is obtained for $\alpha < 5^\circ$ for all the coefficients in the case of Wing 1; thereafter, the nonlinear force of the body leads to significant differences, as seen in Fig. 5. In the case of the smaller-span Wing 8, very poor agreement is obtained for the wing normal-force at both Mach numbers, as seen in Fig. 8, with a significant over prediction in the normal-force slope at $\alpha = 0^\circ$. Considering the good agreement of the SBT prediction of $C_{N_{W(B)}}$ at low α, which is obtained from the experimental C_{N_W}, and considering the significantly better agreement of the WingBody results for Wing 1, it is suggested that the large difference may be attributed to either numerical issues in the code arising from poorly conditioned panels over the majority of the highly swept (85.5°) wing. Similar overprediction in the body normal-force is obtained, as seen in Fig. 6. The results from the WingBody panel code suggest that a simple linear potential-flow method may be suitable to predict the interference and overall loads for $\alpha < 5^\circ$ in the Mach range considered, provided that the leading-edge sweep is not extreme ($\Lambda_{LE} < 80^\circ$). Improved prediction is expected from codes in which the vortex sheet from the wing leading-edge is modelled. The WingBody code provides a significantly better prediction of the body normal-force slope at $\alpha = 0^\circ$ compared to piston theory in both cases and Mach numbers. This is not surprising, as the downwash equation, Eq. (5), is a poor representation of the flow for the low-subsonic crossflow Mach number $M_\infty \sin\alpha$.

4.2 Piston Theory

The aforementioned issue of the downwash equation for the body in piston theory at low-subsonic crossflow Mach numbers is evident in the results for the body normal-force slope at $\alpha = 0^\circ$ in Fig. 5 and Fig. 6. Eq. (5) results in a non-zero lifting pressure on the cylindrical portion of the body for all α; this is inconsistent with the concept of established flow over a cylinder in the crossflow plane at low α, which suggests that only the nose contributes to the normal-force. Isolating the normal-force from the nose alone in Fig. 5 and Fig. 6 shows that good correlation with the nose normal-force from experiment is obtained by 1st-order piston theory for the available data range of $0^\circ \leq \alpha \leq 25^\circ$, with improved agreement at the higher Mach number. Comparison of the slope of the nose-alone normal-force in Fig. 6 from piston theory to the experimental slope for the body in the presence of the wing suggests that for $\alpha < 5^\circ$ the nose-alone prediction serves as an approximation to the overall lift on the body for Wing 8.

Investigation of the results in Fig. 5 and Fig. 6 at high α shows that the impact-like downwash equation, Eq. (9), becomes more appropriate at higher crossflow Mach numbers, as $M_\infty \sin\alpha$ approaches and exceeds unity and the Sychev-regime is approached. The sudden change in slope of the body normal-force noted for 1st-order piston theory arises due to the leeside flow reaching vacuum in the 1st-order model; it is noted that this is delayed when the 3rd-order model is used. It is noted that the normal-force slope from 3rd-order piston theory and from experiment both appear to asymptote to a near-constant value for $\alpha > 15^\circ$, with better agreement at $M_\infty = 2$. From Eq. (4) and Eq. (9) it is seen that for the cylindrical portion of the body, $C_{N_B} \propto c_3 M_\infty \sin^3\alpha$, which differs from the Sychev similarity parameter of $M_\infty \sin\alpha$; thus, the correlation in slopes over the range of α shown at $M_\infty = 2$, as noted for both wing-body combinations, may be a happy coincidence.

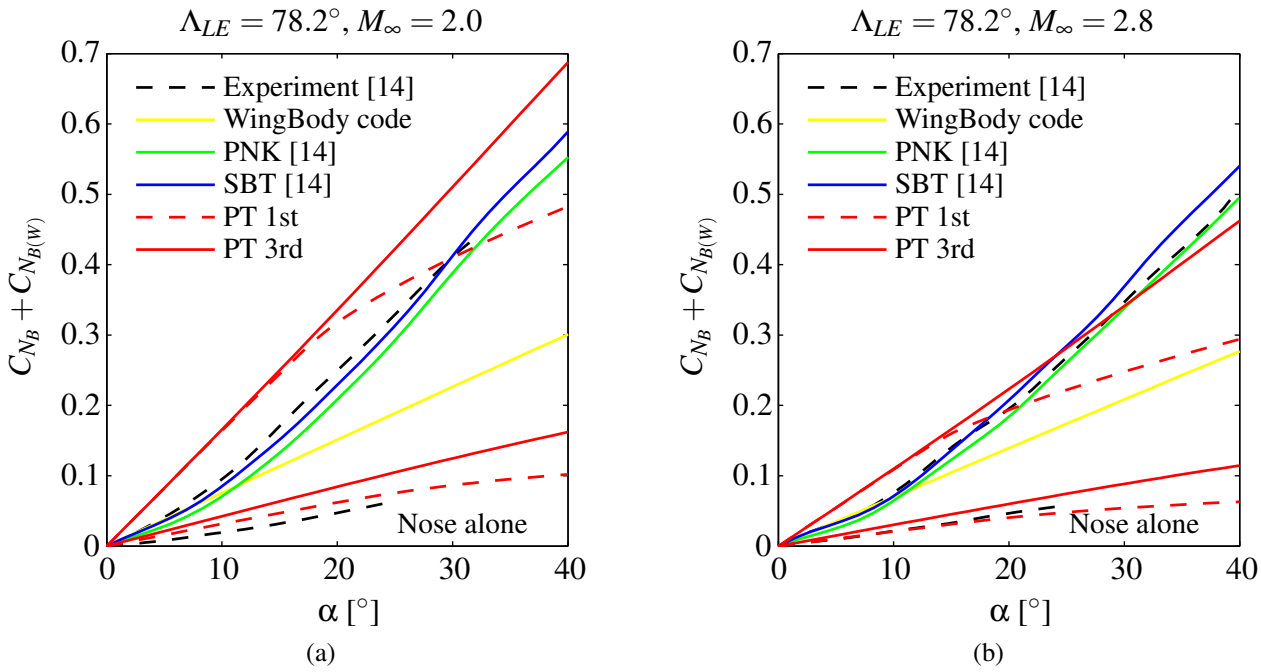

Fig. 5 : Body normal-force coefficient in the presence of Wing-1: (a) $M_\infty = 2.0$, (b) $M_\infty = 2.8$.

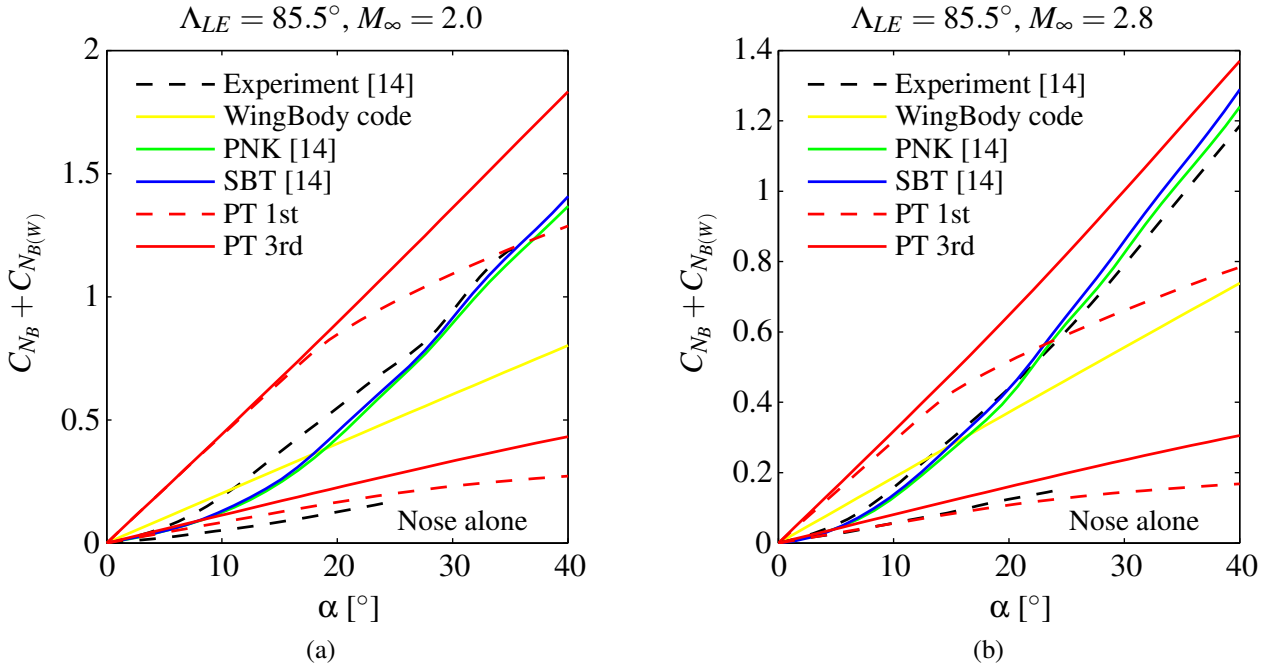

Fig. 6 : Body normal-force coefficient in the presence of Wing-8: (a) $M_\infty = 2.0$, (b) $M_\infty = 2.8$.

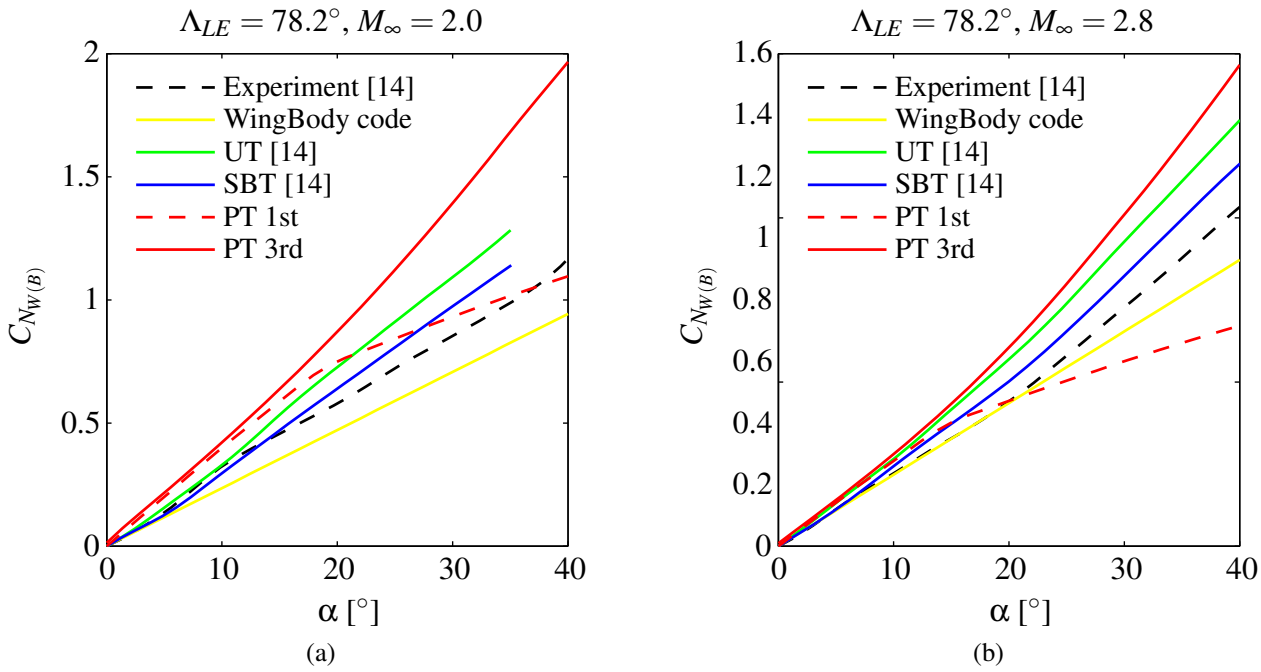

Fig. 7 : Wing-1 normal-force coefficient in the presence of the body: (a) $M_\infty = 2.0$, (b) $M_\infty = 2.8$.

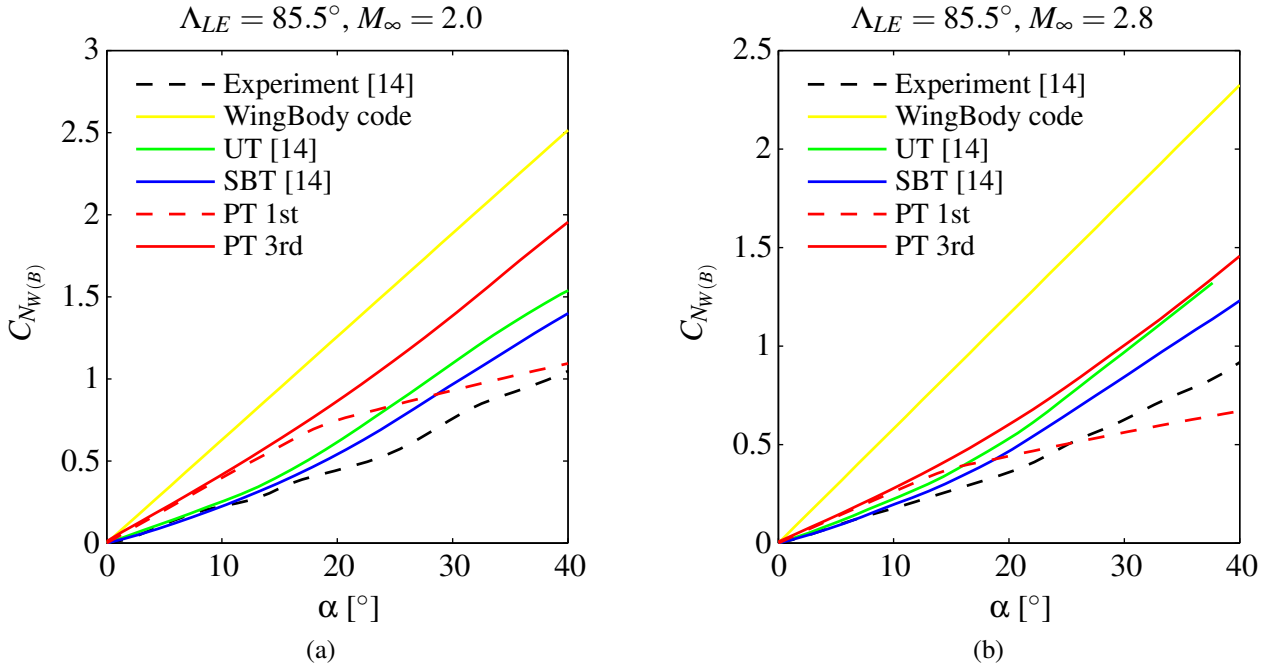

Fig. 8 : Wing-8 normal-force coefficient in the presence of the body: (a) $M_\infty = 2.0$, (b) $M_\infty = 2.8$.

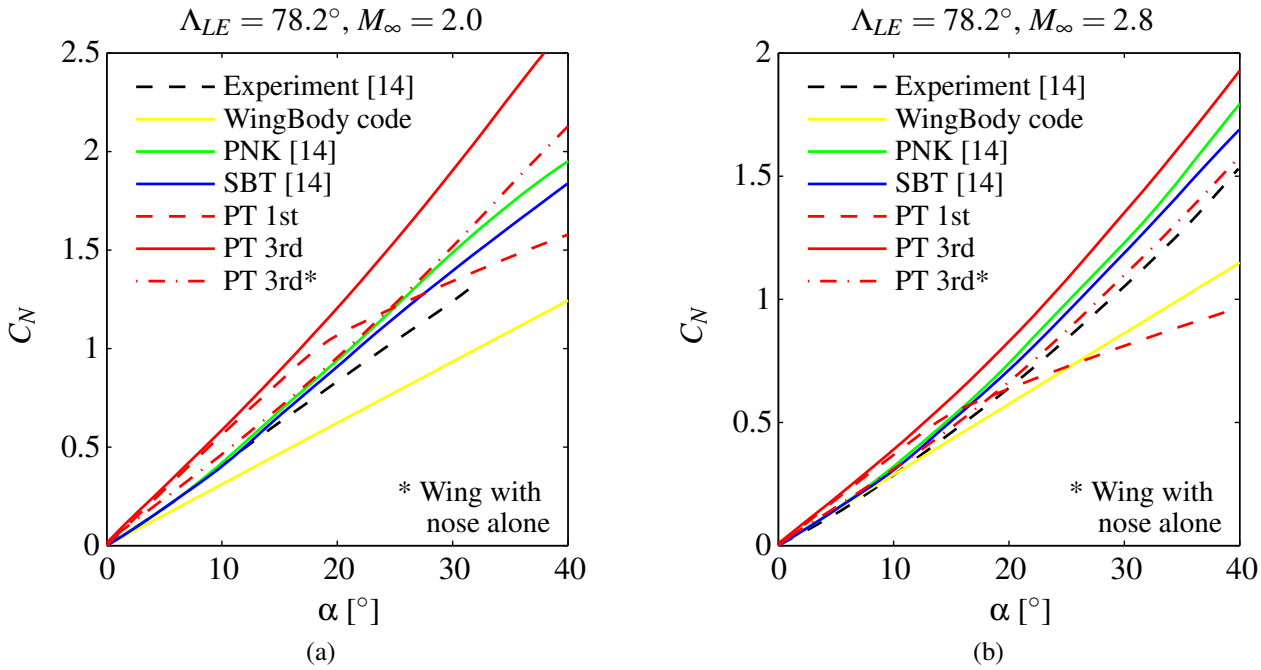

Fig. 9 : Overall normal-force coefficient for the Wing-1-body configuration : (a) $M_\infty = 2.0$, (b) $M_\infty = 2.8$.

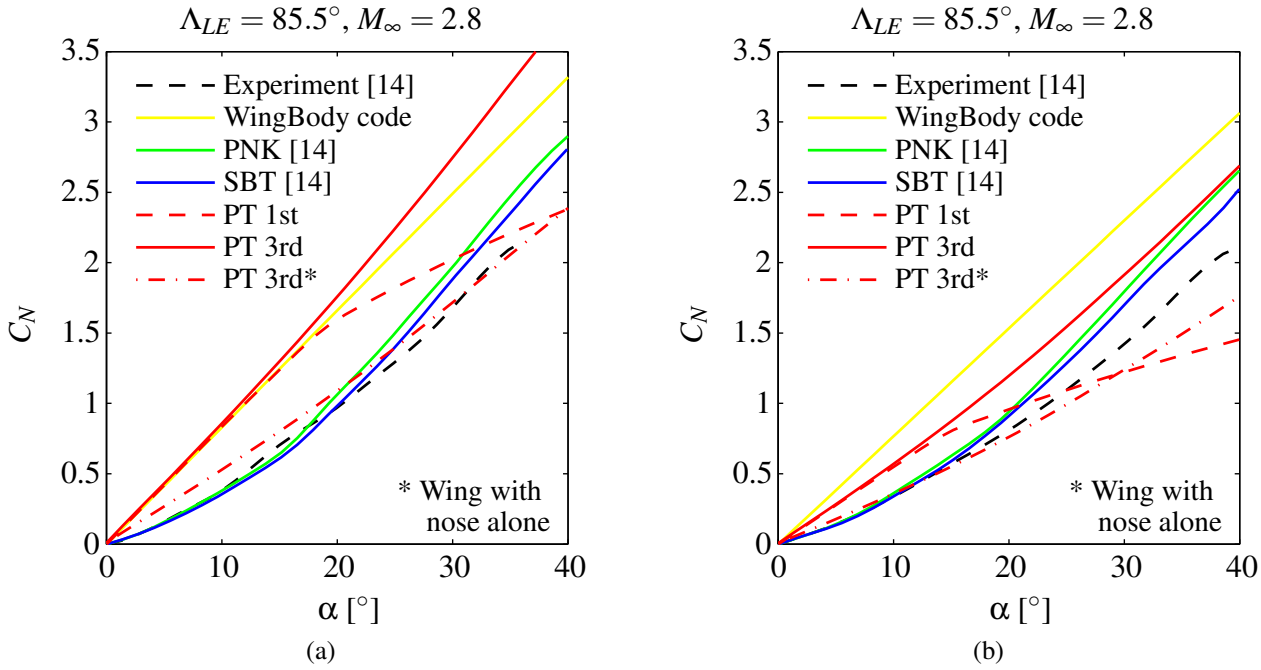

Fig. 10 : Overall normal-force coefficient for the Wing-8-body configuration : (a) $M_\infty = 2.0$, (b) $M_\infty = 2.8$.

Consideration of Figs. 9–10 shows that piston theory consistently over-predicts the wing normal-force slope, with degradation in performance as α increases. The best agreement is obtained at low incidence for the less-swept Wing 1 at the higher Mach number of $M_\infty = 2.8$: this is expected, as this represents the closest combination of parameters to the domain for which piston theory is theoretically valid. Once again, the rapid change in the normal-force slope for 1st-order piston theory is due to vacuum being reached in the 1st-order model. In considering the results for C_{N_W} as predicted by piston theory, it is noted that for the given geometries, thickness effects are negligible and nonlinearities are due to the proportionality $C_{N_W} \propto c_3 M_\infty \sin^3\alpha$. The worse prediction of $dC_{N_{W(B)}}/d\alpha$ at $\alpha = 0^\circ$ noted for Wing 8 relative to Wing 1 is consistent with the smaller portions of the flowfield in which both spanwise and axial gradients may be neglected, as assumed in piston theory.

The preceding comments regarding $C_{N_B} + C_{N_{B(W)}}$ and C_{N_W} as predicted by piston theory are reflected in the results for the overall normal-force (C_N) of the wing-body section, as shown in Fig. 5 and Fig. 6. The prediction by 3rd-order piston theory for the wing-alone and the nose-alone is included to provide an estimate of the improvement to $dC_N/d\alpha$ at $\alpha = 0^\circ$ that might be achieved through more appropriate modelling of the pressure on the cylindrical body at low-subsonic crossflow Mach numbers.

5 Conclusions

The theoretical basis for applying piston theory requires that velocity gradients in two orthogonal directions (one being the axis for the unsteady analogy) be negligible relative to gradients in a third direction (the orientation of the cylinder). Theoretical considerations for the validity of these assumptions suggest that classical piston theory may be applied for $\alpha \approx 0^\circ$ in regions sufficiently far from the wing-body junction and from the wing-tips and at sufficiently high Mach numbers. Outside of these parameters, the flowfield is 2D unsteady in the cross-flow plane and interference must be accounted for. Comparison of piston theory predictions to experimental results for highly swept wing-body combinations suggest that classical piston theory may not be applied without modification; results for the body at high-subsonic to supersonic crossflow Mach numbers suggest preliminary prediction of $dC_N/d\alpha$ may be possible using classical piston theory.

Acknowledgements

This paper is dedicated to Prof. P. G. Karkle, who passed away before the completion of the work.

References

[1] Ashley H and Zartarian G. Piston theory – a new tool for the aeroelastician. *Journal of the Aeronautical Sciences*, Vol. 23, No. 12, pp 1109-1118, 1956.

[2] Dowell EH and Bliss DB. New look at unsteady supersonic potential flow aerodynamics and piston theory. *AIAA Journal*, Vol. 51, No. 9, pp 2278-2281, 2013.

[3] Krumhaar H. The accuracy of linear piston theory when applied to cylindrical shells. *AIAA Journal*, Vol. 1, No. 6, pp 1448-1449, 1963.

[4] Liu DD, Yao ZX, Sarhaddi D and Chavez F. From piston theory to a unified hypersonic-supersonic lifting surface method. *Journal of Aircraft*, Vol. 34, No. 3, pp 304-312, 1997.

[5] McNamara JJ, Crowell AR, Friedmann PP, Glaz B and Gogulapati A. Approximate modeling of unsteady aerodynamics for hypersonic aeroelasticity. *Journal of Aircraft*, Vol. 47, No. 6, pp 1932-1945, 2010.

[6] Zhang WW, Ye ZY, Zhang CA and Liu F. Supersonic flutter analysis based on a local piston theory. *AIAA Journal*, Vol. 47, No. 10, pp 2321-2328, 2009.

[7] Shi X, Tang G, Yang B, Li H. Supersonic flutter analysis of vehicles at incidence based on local piston theory. *Journal of Aircraft*, Vol. 49, No. 1, pp 333–337, 2012.

[8] Han H, Zhang C, Wang F. An approximate model of unsteady aerodynamics for hypersonic problems at high altitude. *Chinese Journal of Theoretical and Applied Mechanics*, Vol. 45, No. 5, pp 690-698, 2013. (Abstract in English)

[9] Ilyushin AA. The law of plane sections in the aerodynamics of high supersonic speeds. *Journal of Applied Mathematics and Mechanics*, Vol. 20, No. 6, 1956.

[10] Sychev VV. Three-dimensional hypersonic gas flow past slender bodies at high angles of attack. *Journal of Applied Mathematics and Mechanics*, Vol. 24, No. 2, pp 296-306, 1960.

[11] Hayes WD and Probstein RF. *Hypersonic inviscid flow*. 1st edition, Dover Publications, 2004.

[12] Voevodenko NV and Panteleev IM. Numerical modeling of supersonic flow over wings with varying aspect ratio on a broad range of angles of attack using the law of plane sections. *Fluid Dynamics*, Vol. 27, No. 2, pp 239-244, 1992.

[13] Meijer MC and Dala L. Piston theory applied to wing-body configurations: a review of the mathematical basis. *READ 2016*, Warsaw, Vol. 1, 2016.

[14] Fellows KA and Carter EC. Results and analysis of pressure measurements on two isolated slender wings and slender wing-body combinations at supersonic speeds: Part 1 – Analysis. *A.R.C. C.P. 1131*, 1970.

[15] Pitts WC, Nielsen JJ and Kaattari GE. Lift and centre of pressure of wing-body-tail combinations at subsonic, transonic and supersonic speeds. *NACA Report 1307*, 1957.

[16] Meijer MC and Dala L. Zeroth-order flutter prediction for cantilevered plates in supersonic flow. *Journal of Fluids and Structures*, Vol. 57, pp 196-205, 2015.

[17] Lighthill MJ. Oscillating airfoils at high Mach number. *Journal of the Aeronautical Sciences*, Vol. 20, No. 6, pp 402-406, 1953.

6 Contact Author Email Address

mariuscmeijer@gmail.com

Copyright Statement